INVESTIGATIONS ON THERMO-HYDRAULIC PERFORMANCE DUE TO ARC ANGLE OF BROKEN ARC RIB COMBINED WITH STAGGERED RIB IN A RECTANGULAR DUCT OF SOLAR AIR HEATER

R S Gill[a], V S Hans[b] and J S Saini[c]

[a] Research scholar, Department of Mechanical Engineering, Guru Nanak Dev Engineering College, Ludhiana, Regional center of Punjab Technical University, Kapurthala, India.

[b] Professor, Department of Mechanical Engineering, Punjab Agricultural University, Ludhiana, India.

[c] Former Professor, Department of Mechanical and Industrial Engineering, Indian Institute of Technology, Roorkee, India.

Abstract:-In this investigation, thermo-hydraulic performance of rectangular ducts roughened with a new configuration of 'broken arc rib combined with staggered rib piece' on one broad wall is determined. The duct has aspect ratio (AR) of 12 and the Reynolds number (Re) ranged from 2000 to 16000. To simulate the indoor testing of solar air heater, the roughened side of rectangular duct is heated with constant heat flux electric heater while the remaining three walls are insulated. These boundary conditions correspond closely to those found in solar air heaters. Five broken arc rib combined with staggered rib roughened plates having arc angle of 15°, 30°, 45°, 60° and 75° have been tested. The relative staggered rib size, relative staggered rib position, relative roughness height, relative gap size, relative gap position and relative roughness pitch were fixed as 4, 0.6, 0.043, 1.0, 0.65 and 10 respectively. The thermo-hydraulic performance parameter based on equal pumping power (η), friction factor (f) and Nusselt number (Nu), are found to be more at arc angle (α) of 30° than at other arc angles. The highest value of thermo-hydraulic performance is 2.33 corresponding to Reynolds number of 12000.

***Keywords*: Solar air heater, staggered rib, arc-angle, Nusselt number, friction factor, rib roughness**

1. Introduction

The thermal performance of conventional solar air heaters is significantly enhanced by the use of artificial rib roughness on the underside of absorber plate due to restriction caused in development of viscous and thermal boundary layer. But the increase in heat transfer is accompanied by increase in friction power penalty. Early studies on heat transfer and friction factor relates to ducts roughened with transverse ribs (Han et al., 1978). It was then found that placing the ribs at an angle to the main stream flow will result in greater heat transfer than ribs positioned at 90° to the mainstream flow. Studies by Han and Park (1988) and Park et al. (1992) investigated the thermal performance of angled ribs. The results showed the heat transfer enhancement in angled rib channels is significantly greater than the heat transfer enhancement due to orthogonal ribs. With the focus of rib roughness shifted to high performance ribs, Han et al. (1991) studied continuous V-up and V-down ribs and Hans (2010) studied continuous multi V-shape ribs. The result of these studies has shown that the continuous V-shape and multi V-shape ribs perform better than inclined rib due to generation of more counter rotating secondary flow cells relative to inclined rib. Further, it was shown that gap in continuous inclined rib (Aharwal, 2009), gap in continuous V-rib (Singh et al., 2011) and gap in continuous multiple V-rib (Kumar et al., 2013) further enhance the heat transfer due to generation of more number of secondary flow cells and interruption of growth of boundary layer downstream of a rib as secondary flow passes through the gap (Cho et al., 2003). In order to achieve further enhancement in heat transfer, Patil et al. (2012) introduced staggered rib piece in the inter-rib space of V-ribs with gap, Kumar and Kim (2015), Deo et al. (2016), Jin et al. (2017) and Patel and Lanjewar (2018) introduced staggered rib piece in multi V-down ribs and reported significant improvement in thermo-hydraulic performance. The heat transfer enhancement was found to be influenced by the introduced staggered rib piece scheme.

The past studies have shown that gap in V-ribs perform better than continuous V-ribs, and which in-turn performs better than angled or orthogonal ribs. Besides, the studies have also shown that introduction of staggered rib piece in the inter-rib space of ribs with gap perform better (Patil et al., 2012; Kumar and Kim, 2015; Deo et al., 2016; Jin et al., 2017; Patel and Lanjewar, 2018). The previous studies (Cho et al., 2003; Aharwal et al. 2009; Patil et al., 2012; Deo et al., 2016) have also shown that the friction factor and Nusselt number of the roughened duct are strong function of rib angle (α). The past studies have shown that that still no study is available on optimization of arc angle in case of broken arc rib roughness combined with staggered rib piece roughness geometry for solar air heater. It appears fruitful to investigate the effect of variation in arc angle (α) of broken arc shaped ribs combined with staggered rib piece roughness geometry. Therefore, the present study has been taken up to explore the effect of arc angle on the heat transfer and friction in a high aspect ratio solar air heater duct roughened with broken arc rib roughness combined with staggered rib piece. Experimentations have been conducted in the Reynolds number range of 2000-16000 to generate data pertaining to heat transfer and friction for fully developed turbulent flow through an artificially roughened solar air heater duct. Based on data generated, the variation of Nusselt numbers, friction factors and thermo-hydraulic performance parameter of the system as function of arc angle have been determined to ensure the benefit of roughness geometry

selected in this study. In the following sections, rib roughness geometry, range of parameters, experimental details, data reduction and results are presented and discussed in the following sections.

2. Rib roughness geometry and range of parameters

Fig.1 shows the general geometry of broken arc rib combined with staggered rib roughness. The investigation was carried out to determine the Nusselt number and friction factor due to change in angle of attack (α). Five roughened plates were prepared for arc-angle (α) of 15°, 30°, 45°, 60° and 75°. The other roughness parameter i.e. relative staggered rib size (r/g), relative staggered rib position (p'/p), relative roughness height (e/D_h), relative gap size (g/e), relative gap position (w'/w), and relative roughness pitch (p/e) were kept fixed as 4, 0.4, 0.043, 1.0, 0.65, and 10 respectively. Artificial rib roughness was created by fixing aluminium wires of circular cross-section on the underside of absorber plates of solar air heater duct. The Reynolds number was varied from 2000 to 16000 (8 levels).

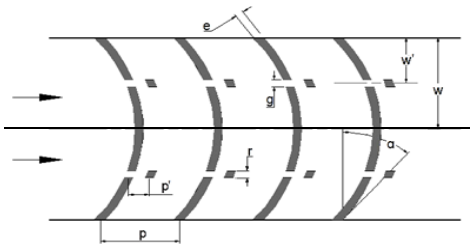

Fig. 1: Roughness geometry

3. Experimental Details

3.1. Experimental Setup

An experimental test facility has been designed and fabricated to study the effect of arc angle of broken arc rib combined with staggered rib geometry on the heat transfer and fluid flow characteristics of a rectangular duct. A schematic diagram of experimental setup is shown in Fig. 2. It consists of an entry section, a test section, an exit section, a flow meter and a centrifugal blower. The rectangular duct has a flow cross-section of 300 mm x 25 mm. The length of entry section, test section and exit section is 5500 mm, 1000 mm and 890 mm respectively. The recommended minimum entry and exit length is 5 √WH and 2.5 √WH respectively (ASHRAE standards 93-77, 1977). Therefore, the flow can be assumed to be fully developed in the entire test section length. A longer exit section (890 mm length) is provided in order to minimize the end effects. The top side of the test section is 1 mm thick galvanized iron (GI) sheet. 1 mm thick galvanized iron sheet having artificial roughness is used as the top broad wall of the rectangular duct. The inner surface of remaining three sides of duct is also smooth sunmica. The absorber plate is heated from the top by supplying uniform heat flux (1000 W/m^2) by means of an electrical heater. In order to minimize the heat loss from the topside of the heater assembly, the electric heater is fitted over a box made of 12 mm thick plywood, of size 2440 mm×390 mm×100 mm. The hollow inner space of the heater box is filled with glass wool (i.e. 76 mm thick). The complete duct is further insulated with 50 mm thick polystyrene insulation having thermal conductivity of 0.037 W/m K to minimize heat loss to the environment. The mass flow rate of air through the duct was measured by means of a calibrated orifice meter (calibrated against a standard Pitot tube) in the flow line connected with an inclined U-tube manometer, and the flow was controlled by the control valve provided. Calibrated thermocouples, prepared by butt welding of 0.3-mm-diameter copper–constantan wires were used for temperature measurement. Nineteen thermocouples were used to measure the temperature of top surface of the absorber plate at different locations. Five thermocouples were arranged span wise in the duct to measure the air temperature after the mixing section and one thermocouple was used to determine the inlet air temperature. A digital temperature indicator was used for the output of the thermocouples. The pressure drop across the test section was measured by digital micro-manometer of least count 0.001 Pa.

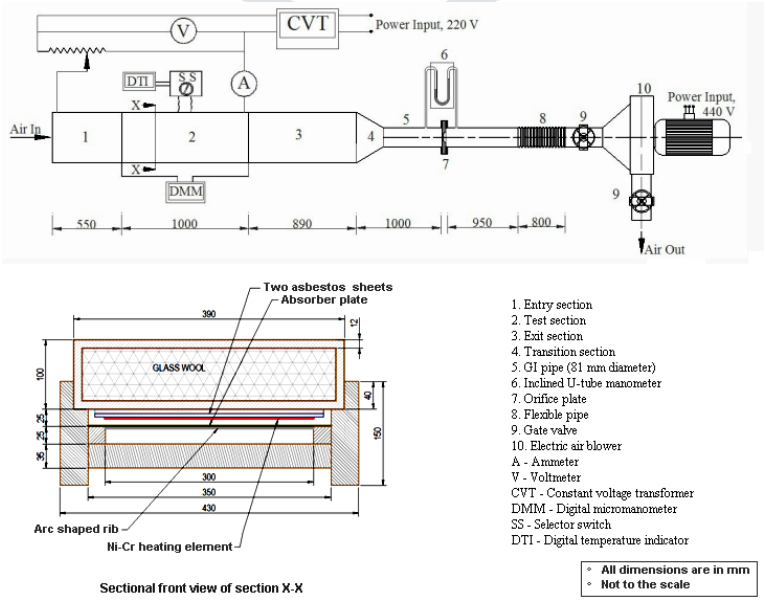

Fig. 2 Schematic of experimental setup

3.2. Experimental Procedure

The experimental data on rib roughened duct pertaining to heat transfer and flow friction was collected in accordance with recommendation of ASHRAE Standard 93-77 (1977) for testing of solar collectors operating in open loop flow mode. The roughened plates having different values of arc angles were tested. In order to compare the results of the roughened duct with that of smooth duct, a smooth plate operating under similar flow conditions was also tested. At the start of each set of experiment, it was ensured that all instruments were working properly and there was no leakage at the joints. All the data was collected under steady state conditions. For each set, at the start it takes 2-3 hours to reach a steady state. The steady state was assumed to have been attained when no considerable variation in plate temperature and outlet air temperatures was observed over a period of 10 minutes. The parameters recorded for each set of experiment were inlet air temperature, outlet air temperature at five points in the span-wise direction of the duct, temperature of the heated plate at nineteen locations, pressure drop across the orifice plate and pressure drop across the test section.

4. Data Reduction

Mass flow rate (m) of air has been determined from the pressure drop across the orifice plate using the following relation:

$$m = C_d A_o \left[\frac{2\rho_{air}(\Delta P_o)}{1-\beta^4} \right]^{0.5} \quad (1)$$

The heat transfer rate to the air is calculated as:

$$Q_u = mC_p(T_o - T_i) \quad (2)$$

The heat transfer coefficient for the test section is calculated as:

$$h = \frac{Q_u}{A_p\left(T_{pm} - T_{fm}\right)} \quad (3)$$

The Nusselt number is calculated from the heat transfer coefficient (h) using the following relation:

$$Nu = \frac{hD_h}{K_{air}} \quad (4)$$

The friction factor (f) is determined from the measured values of pressure drop across the length (L_f) of 1m in the test section using the equation:

$$f = \frac{2(\delta P)\rho_{air} D_h}{4L_f G_{air}^{\ 2}} \quad (5)$$

The thermo-physical properties of air used in the calculations corresponds to bulk mean air temperature.

5. Validity Test

For validation of experimental setup, the Nusselt number and friction factor for smooth duct were determined from experimentation on smooth duct and their values compared with the values calculated from the correlations for smooth duct available in literature. The values of the Nusselt number and friction factor for a smooth rectangular duct is calculated from the Dittus–Boelter equation (Rohsenow et al., 1998) and modified Blasius equation (Bhatti and Shah, 1987) given below in Eq. (6) and Eq. (7) respectively.

$$Nu_s = 0.023\,\mathrm{Re}^{0.8}\,\mathrm{Pr}^{0.4} \quad (6)$$

$$f_s = 0.085\,\mathrm{Re}^{-0.25} \quad (7)$$

The comparison of experimental and predicted values of Nusselt number and friction factor is shown in Figs. 3 and 4. The average absolute deviation of experimental values of Nusselt number is ±3.9% from the values predicted by Eq. (6), and the average absolute deviation of experimental values of friction factor is ±2.5% from the values predicted by Eq. (7). Thus, a reasonably good agreement between the predicted and experimental values ensures the accuracy of the experimental data collected with the present experimental set-up.

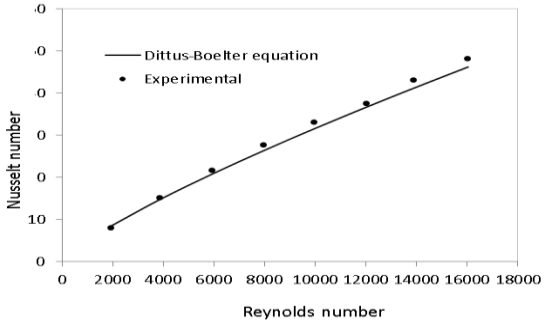

Fig. 3. Comparison of experimental and predicted values of Nusselt number (Nu_s) for smooth duct.

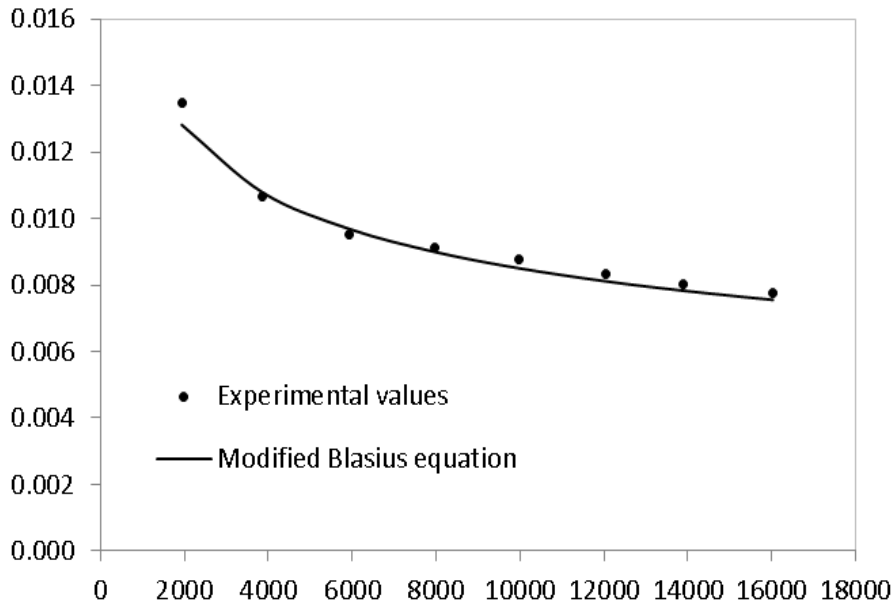

Fig. 4. Comparison of experimental and predicted values of friction factor (f_s) for smooth duct.

6. Results and Discussion

Figs. 5 and 6 show the variation of Nusselt number and friction factor with Reynolds number for different values of angle of attack (α). It can be seen that for all Reynolds number as the arc angle increases from 15° to 30°, the Nusselt number and friction factor increase and the both decrease with further increase in arc angle from 30° to 75°. This variation in Nusselt number and friction factor is due to interaction of boundary layer on upstream side of the rib and secondary flow along the rib. The boundary layer is due to main flow with the roughened surface and originates from flow reattachment point between the ribs up to the succeeding downstream rib. The strength of secondary flow along the rib changes with change in arc angle of rib. These two factors determine the value of Nusselt number and friction factor at different values of arc angle. The results agree with earlier study on V-down rib by Han et al. (1991) and Singh et al. (2011).

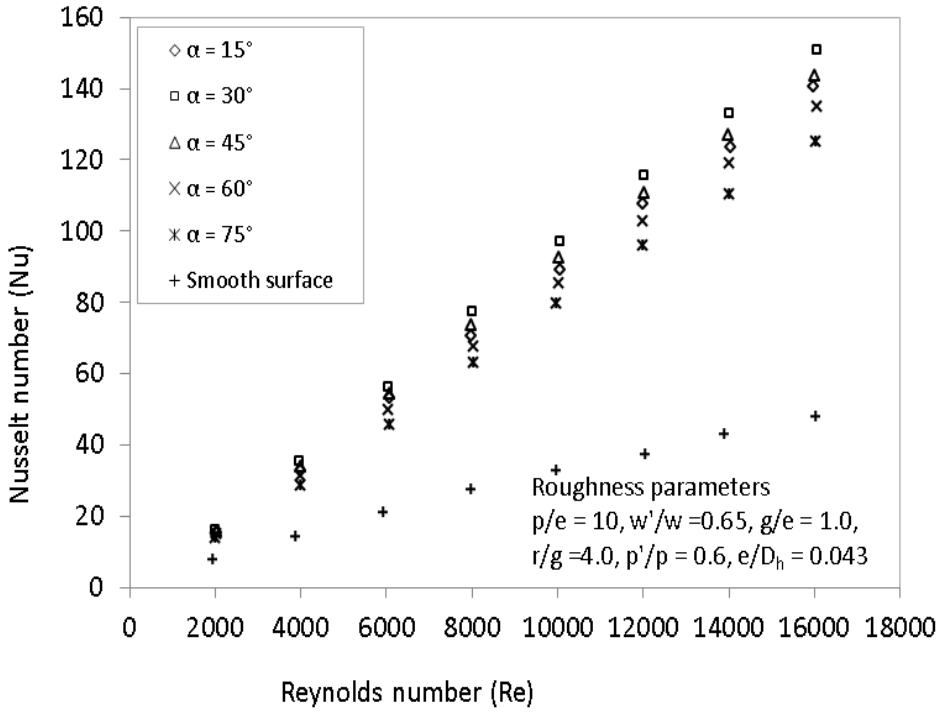

Fig. 5. Variation of Nusselt number with Reynolds number for different values of arc angle (α).

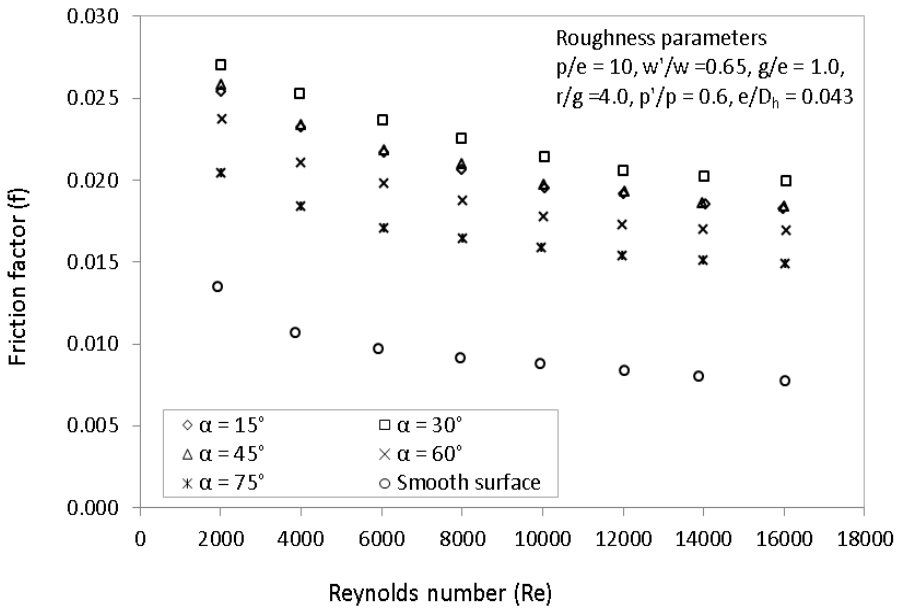

Fig. 6. Variation of friction factor with Reynolds number for different values of arc angle (α).

It can also be seen from Fig. 5 and Fig. 6 that the solar air heater duct roughened with broken arc rib combined with staggered rib piece result in higher Nusselt number as well as friction factor as compared to smooth conventional solar air heater duct. So a performance parameter needs to be determined that takes into account both Nusselt number and friction factor to evaluate the effectiveness of rib roughened surface. A thermo-hydraulic performance parameter based on equal pumping power (η) defined by Webb and Eckert (1972) takes into account both the Nusselt number and friction factor enhancement. It is defined as:

$$\eta = \frac{(Nu/Nu_s)}{(f/f_s)^{1/3}} \qquad (8)$$

The value of this parameter greater than unity indicates it is overall advantageous to use roughened surface as compared to smooth surface. Fig. 7 shows a plot of this parameter as a function of Reynolds number at different arc angles for broken arc rib combined with staggered rib. For all angles of attack, the value of α is more than unity. Hence the performance of broken arc rib combined with staggered rib roughened solar air heater duct is better as compared to smooth duct. The thermo-hydraulic performance parameter is more for arc angle of 30° for the range of Reynolds number investigated, thereby indicating that it is advantageous to use broken arc rib combined with staggered rib roughened solar air heater with 30° arc angle as compared to other arc angles. The highest value of thermo-hydraulic performance parameter obtained is 2.33 at Re = 12,000.

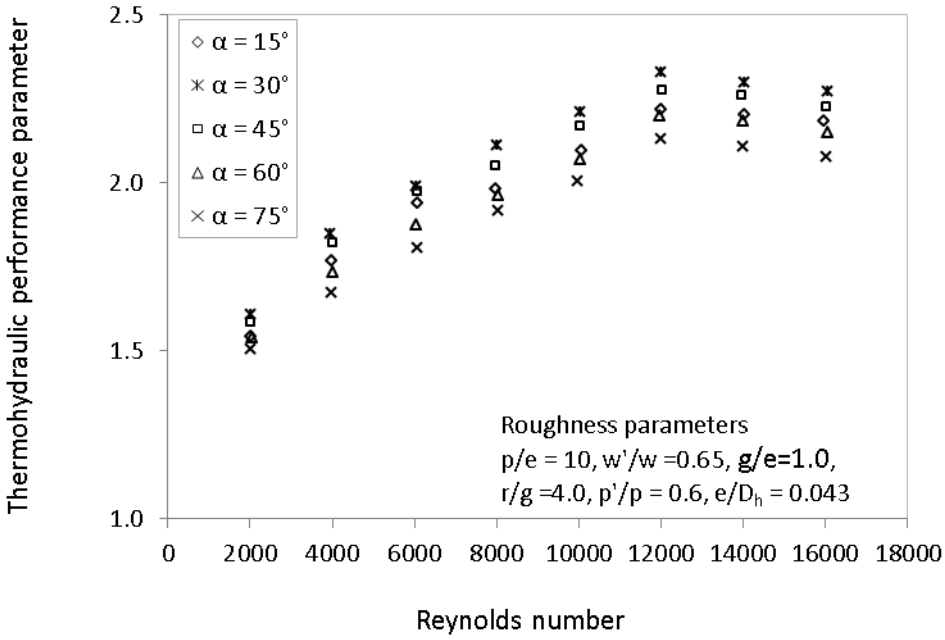

Fig. 7. Variation of thermo-hydraulic performance parameter with Reynolds number for different values of arc angle (α).

7. Conclusions

Based on the experimental investigation on broken arc rib combined with staggered rib roughened solar air heater duct for different arc angles, following conclusions can be drawn:

i. The variation in arc angle has strong influence on Nusselt number and friction factor.

ii. For all Reynolds number, the Nusselt number and friction factor increases with arc angle from 15° to 30° and both decreases with further increase in arc angle from 30° to 75°.

iii. The thermo-hydraulic performance parameter indicates that it is advantageous to use broken arc rib combined with staggered rib roughened solar air heater with arc angle of 30° as compared to other values of arc angles and smooth surface. The highest value of thermohydraulic performance parameter is 2.33 at Reynolds number of 12000.

Nomenclature

A_p absorber plate area, m^2
A_o cross-section area of the orifice, m^2
C_d coefficient of discharge of orifice
C_p specific heat of air at constant pressure, J/kg K
D_h hydraulic diameter of duct, m
e rib height, m
e/D_h relative roughness height
f friction factor of roughened duct
f_s friction factor of smooth duct
G_{air} mass velocity of air, kg/s m^2
h convective heat transfer coefficient, W/m^2K
H duct depth, m
K_{air} thermal conductivity of air, W/m K
L_f test section length for pressure drop measurement, m
m mass flow rate of air, kg/s
Nu Nusselt number of roughened duct
Nu_s Nusselt number of smooth duct
P pitch of the rib, m
P/e relative roughness pitch
Pr Prandtl number of air
Q_u heat transfer rate to air, W
Re Reynolds number
T_{fm} bulk mean air temperature, °C
T_i inlet air temperature, °C
T_o average outlet air temperature, °C
T_{pm} mean plate temperature, °C
W width of duct, m
α angle of attack, °
ΔP_o pressure drop across orifice plate, N/m^2
ΔP pressure drop across length L_f, N/m^2
ρ_{air} density of air, kg/m3
β ratio of orifice diameter to pipe diameter

Acknowledgement

The author acknowledges the Punjab Technical University (PTU), Kapurthala, India for supporting this research work and Punjab Agricultural University (PAU), Ludhiana, India for providing facilities for experimentation.

References

[1] Aharwal, K.R., Gandhi, B.K., Saini, J.S., 2009. Heat transfer and friction characteristics of solar air heater ducts having integral inclined discrete ribs on absorber plate, Int. J. Heat and Mass Transfer, 52 5970–5977.
[2] ASHRAE Standard 93–97, 1977. Method of Testing to Determine the Thermal Performance of Solar Collector. American Society for heating, Refrigeration and Air conditioning Engineering, New York: 1-34.
[3] Bhatti, M.S., Shah, R.K., 1987. Turbulent and transition flow convective heat transfer, in Kakac S, Shah RK, Aung W. (Eds.), Handbook of single-phase convective heat transfer, Chap. 4. John Wiley and Sons, New York.
[4] Cho HH, Kim YY, Rhee DH, Lee S Y, Wu S J, Choi C, 2003. The effect of gap position in discrete ribs on local heat mass transfer in a square duct. J. of Enhanced Heat Transfer, 10: 287-300.
[5] Deo NS, Chander S, Saini JS, 2016. Performance analysis of solar air heater duct roughened with multigap V-down ribs combined with staggered ribs. Renewable Energy, 91: 484-500.
[6] Han JC, Zhang YM, Lee CP, 1991. Augmented heat transfer in square channels with parallel, crossed, and V-shaped angled ribs. Trans ASME J Heat Transfer, 113: 590–596.
[7] Han, J.C., Glicksman, L.R., Rohsenow, W.M., 1978. International Journal of Heat and Mass Transfer, 21; 1143-1156.
[8] Han, J.C.,Park, J.S., 1988. International Journal of Heat and Mass Transfer, 31; 183-195.
[9] Hans VS, Saini RP, Saini JS. 2010. Heat transfer and friction factor correlations for a solar air heater duct roughened artificially with multiple V ribs. Sol Energy, 84: 898–911.
[10] Jin D., Jianguo Z., Quan S., Xu S., Gao H., 2017. Thermohydraulic performance of solar air heater with staggered multiple V-shaped ribs on the absorber plate, Energy, 127: 68-77.
[11] Kumar A., R.P. Saini, J.S. Saini, 2013. Development of correlations for Nusselt number and friction factor for solar air heater with roughened duct having multi v-shaped with gap rib as artificial roughness, Renew. Energy, 58; 151-163.
[12] Kumar Anil and Kim Man-Hoe, 2015. Effect of roughness width ratios in discrete multi V-rib with staggered rib roughness on overall thermal performance of solar air channel. Solar Energy, 119: 399-414.
[13] Park, J.S., Han, J.C., Huang, Y., Ou, S.,Boyle, R.J., 1992. International Journal of Heat and Mass Transfer 35, 2891-2903.
[14] Patel S. S., Lanjewar A., 2018. Experimental analysis for augmentation of heat transfer in multiple discrete V-patterns combined with staggered ribs solar air heater, Renewable Energy Focus, 25: 31-39.
[15] Patil, A. K., Saini J. S., Kumar K., 2012. Nusselt number and friction factor correlations for solar air heater duct with broken V-down ribs combined with staggered rib roughness. Journal of Renewable and Sustainable Energy, 4(3): 033122.
[16] Rohsenow, W.M., Hartnett, J.P., Cho, Y.I., 1998. Hand book of heat transfer. McGraw Hill, New York.
[17] Singh S., Chander S., Saini J.S., 2011. Thermo-hydraulics of solar air heater ducts with discrete V-down rib roughness. International Conference on Renewable Energy, Jaipur, India, 907–912.
[18] Webb, R. L. and E. R. G. Eckert, 1972. Application of rough surface to heat exchanger design. International Journal of Heat and Mass Transfer, 15: 1647–58.